

Technical report 14-006

On a Spatiotemporally Discrete Urban Traffic Model*

S. Lin, B. De Schutter, A. Hegyi, Y. Xi, and J. Hellendoorn

To cite this work, please refer to the published version:

S. Lin, B. De Schutter, A. Hegyi, Y. Xi, and J. Hellendoorn, “On a spatiotemporally discrete urban traffic model,” *IET Intelligent Transport Systems*, vol. 8, no. 3, pp. 219–231, May 2014. doi:[10.1049/iet-its.2012.0137](https://doi.org/10.1049/iet-its.2012.0137)

Delft Center for Systems and Control
Delft University of Technology
Mekelweg 2, 2628 CD Delft
The Netherlands
phone: +31-15-278.24.73 (secretary)
URL: <https://www.dcsc.tudelft.nl>

* This report can also be downloaded via <https://dpub.eu/14-006>

On a spatiotemporally discrete urban traffic model

S. Lin^{*,*}, B. De Schutter[†], A. Hegyi[◇], Y. Xi^{*}, J. Hellendoorn[†]

^{*} School of Computer and Control Engineering, University of Chinese Academy of Sciences,
No. 80 ZhongGuanCunDongLu, HaiDian, Beijing 100190, China
Email: lisashulin@gmail.com

^{*} Department of Automation, Shanghai Jiao Tong University,
and Key Laboratory of System Control and Information Processing, Ministry of Education of China,
No. 800 Dongchuan Road, Minhang District, Shanghai 200240, China
Email: ygxi@sjtu.edu.cn

[†] Delft Center for Systems and Control, Delft University of Technology
Mekelweg 2, 2628 CD Delft, The Netherlands
Email: {b.deschutter, j.hellendoorn}@tudelft.nl

[◇] Department of Transport and Planning, Delft University of Technology
PO Box 5048, 2600 GA Delft, The Netherlands
Email: a.hegyi@tudelft.nl

Abstract

In order to control urban traffic with model-based control methods, a proper traffic model is very important. This traffic control model needs to have enough descriptive power to reproduce relevant traffic phenomena, and it also has to be fast enough to be used in practice. Consequently, macroscopic urban traffic flow models are usually applied as control models. In this paper, a macroscopic spatiotemporally discrete urban traffic model with a variable sampling time interval is proposed for model-based control strategies. By selecting proper sampling time intervals and sampling space distances, it allows to balance modeling accuracy and computational complexity of the spatiotemporally discrete model. In addition, an urban traffic CFL (Courant-Friedrichs-Lewy) condition is deduced for spatiotemporally discrete urban traffic models, which is a sufficient condition to guarantee the discrete model to bear enough descriptive modeling power to reproduce necessary traffic phenomena. The model is analyzed and evaluated based on the model requirements for control purposes. The simulation results are compared for the situations that the CFL condition is violated and not violated.

1 Introduction

Traffic models can be mainly classified into three categories based on the modeling details: microscopic models, macroscopic models, and mesoscopic models [1]. Microscopic models are detailed traffic models that describe the dynamics of each individual vehicle, like car-following models. In contrast,

macroscopic models are much rougher models focusing only on the dynamics of traffic flows, i.e. the average behavior of groups of vehicles instead of individual vehicles. Mesoscopic models combine both the properties of the microscopic models and the macroscopic models. Macroscopic traffic models are often used in model-based traffic management, e.g. traffic control, traffic flow estimation and prediction, where the traffic is managed at a macroscopic level and high real-time computing efficiency is required. A first-order macroscopic model was proposed in [2] to describe the dynamics of traffic flows, and it was extended into second-order macroscopic models in [3]. But, this model was criticized for not being able to reproduce enough descriptive accuracy for modeling the phenomena of real traffic in [4]. In general, macroscopic models are approximations of traffic dynamics, and they ignore some details of individual vehicles and make many simplifications, so macroscopic traffic models are in general not as accurate as models with a higher level-of-detail. However, this statement does not always hold in practice. On some occasions, macroscopic modeling approaches may provide better results than modeling approaches with a higher level-of-detail [1], since a more detailed traffic model may accumulate even more errors. Therefore, a proper macroscopic traffic model will be a good choice for the traffic applications that are characterized by high computational requirements, such as traffic control. Macroscopic models can also exhibit various level-of-details. For traffic control purposes, we need to select suitable macroscopic traffic models with proper modeling accuracy and limited computational burden. When selecting a suitable model, we need to follow a criterion [5], which is the model should have sufficient descriptive power to reproduce all important phenomena for traffic control, and at the same time the execution speed of a simulation should be fast enough according to the control requirements. Therefore, we need to find a trade-off between the descriptive accuracy of the model and the computational complexity.

In urban areas, the traffic flows are influenced a lot by the traffic signals. Therefore, the store-and-forward model [6] was proposed to describe the stop-and-go traffic flow dynamics controlled by the traffic signals for urban roads. The store-and-forward model, later used for control in [7], is a simple model with a low computational complexity, but it only applies for saturated traffic, i.e. when the vehicle queues resulting from the red phase cannot be dissolved completely at the end of the following green phase. This model is further extended in [8] to describe different traffic scenarios, i.e. unsaturated, saturated, and over-saturated traffic scenarios. The model proposed in [9] and extended in [10] can describe vehicle queues and the time delay for vehicles reaching the queues in a link. The cell transmission model [11] and the link transmission model [12, 13] are both models based on kinematic wave theory by Lighthill and Whitham [2], and Richards [14]. These two models are also spatiotemporally discrete traffic models. The model proposed in [15] has a lower modeling power, but cannot describe scenarios other than saturated traffic either. The model of [16–19] is capable of simulating the evolution of traffic dynamics (including vehicle queues) in all traffic scenarios (unsaturated, saturated, and over-saturated traffic conditions) by updating the discrete-time model in small simulation steps. To reduce the computational complexity of this model, a model with a longer sampling time interval was proposed in [20, 21]. This model is much faster than the previous model, with only a limited loss in modeling accuracy. Actually, all the macroscopic urban traffic models mentioned above are spatiotemporally discrete models, which are spatially sampled into road segments and temporally sampled with a sampling time interval. But, there is still a lack of research on how the sampling time interval and the sampling space distance will influence the modeling accuracy and the computational complexity of the sampled urban traffic models.

In this paper, a spatiotemporally discrete urban traffic model is proposed for use in model-based traffic control strategies. This model is derived by sampling a queue-based first-order continuous traffic

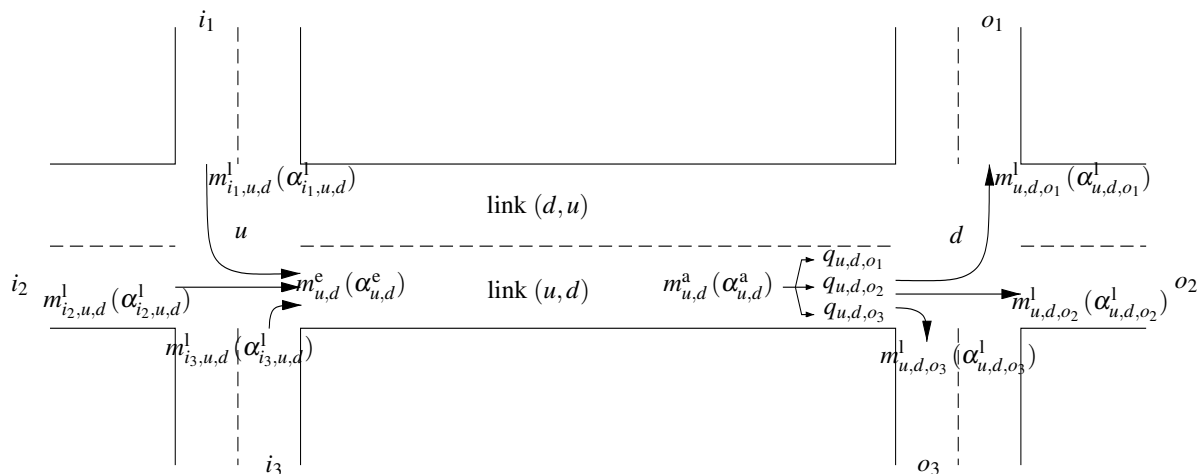


Figure 1. A link connecting two traffic-signal-controlled intersections

flow model spatially and temporally. For spatiotemporally discrete models of urban traffic networks, the roads are comparatively short and divided by intersections with traffic signals, and thus the entire urban roads are usually taken as the sampled road segments, i.e. the sampling space distance is considered as the link length. But, the sampling time interval of the model proposed in this paper can vary freely according to the control requirements. Normally, a higher sampling frequency results in a more accurate model, but also gives rise to more computations because of having to update the model more frequently. Varying the sampling time interval allows to balance the modeling accuracy and the computational complexity of the spatiotemporally discrete model. When the sampling time interval becomes too large, the spatiotemporally discrete model cannot represent the continuous traffic flow behavior anymore. Therefore, an additional criterion (Courant-Friedrichs-Lewy (CFL) condition [22]) needs to be satisfied when sampling urban traffic model into the spatiotemporally discrete model, so as to keep the descriptive ability of the model. An urban traffic CFL condition is deduced in this paper, as a guideline for selecting the sampling time interval and the sampling space distance of the spatiotemporally discrete urban traffic model. This CFL condition can guarantee that the spatiotemporally discrete urban traffic model exhibits enough descriptive ability. Experiments are designed to verify whether the model has sufficient descriptive power to reproduce important traffic phenomena from a control point of view under the situations that the CFL condition is violated and not violated, and whether the computation speed of the model is also fast enough.

This paper is organized as follows. Section 2 proposes the spatiotemporally discrete urban traffic model. Section 3 provides a proof for the discrete-time delay of the model. The CFL condition is deduced for spatiotemporally discrete urban traffic models in Section 4. Section 5 presents the simulation results, and Section 6 concludes the paper.

2 Spatiotemporally discrete urban traffic model

In this section, we derive a spatiotemporally discrete urban traffic model with a variable sampling time interval. In order to describe the model, we define J as the set of nodes (intersections), and L as the set of links (roads) in the urban traffic network. Link (u, d) is marked by its upstream node u ($u \in J$) and downstream node d ($d \in J$). The sets of the upstream nodes of input links and downstream

nodes of output links for link (u, d) are $I_{u,d} \subset J$ and $O_{u,d} \subset J$ (e.g., for the situation of Fig. 1 we have $I_{u,d} = \{i_1, i_2, i_3\}$ and $O_{u,d} = \{o_1, o_2, o_3\}$). The variables used in the model are listed as follows (see also Fig. 1):

$I_{u,d}$: set of upstream nodes of input links of link (u, d) ,
$O_{u,d}$: set of downstream nodes of output links of link (u, d) ,
k	: simulation step counter for the urban traffic model,
$n_{u,d}(k)$: number of vehicles in link (u, d) at simulation step k ,
$q_{u,d}(k)$: queue length (expressed as the number of vehicles) at step k in link (u, d) , $q_{u,d,o}(k)$ is the queue length of the sub-stream turning to link (d, o) ,
$S_{u,d}(k)$: available storage space of link (u, d) at step k expressed in number of vehicles,
$\alpha_{u,d}^l(k)$: average flow rate leaving link (u, d) at step k , $\alpha_{u,d,o}^l(k)$ is the leaving average flow rate of the sub-stream going towards link (d, o) ,
$\alpha_{u,d}^a(k)$: average flow rate arriving at the tail of the queue in link (u, d) at step k , $\alpha_{u,d,o}^a(k)$ is the arriving average flow rate of the sub-stream going towards link (d, o) ,
$\alpha_{u,d}^e(k)$: average flow rate entering link (u, d) at step k ,
$\beta_{u,d,o}(k)$: fraction of the traffic in link (u, d) anticipating to turn to link (d, o) at step k ,
$\mu_{u,d,o}$: saturation flow rate leaving link (u, d) turning to link (d, o) ,
$g_{u,d,o}(k)$: green time length during step k for the traffic stream towards link (d, o) in link (u, d) ,
$v_{u,d}^{\text{free}}$: free-flow vehicle speed in link (u, d) ,
$C_{u,d}$: capacity of link (u, d) expressed in number of vehicles,
$N_{u,d}^{\text{lane}}$: number of lanes in link (u, d) ,
$\Delta C_{u,d}$: offset between node u and node d , which represents the offset time between the cycles of the upstream and the downstream intersections at the beginning of every control time step,
l_{veh}	: average vehicle length.

2.1 Traffic dynamics on a link

Denote the sampling time interval for intersection $d \in J$ and all the links that connect to intersection d by T_d and let k_d is the corresponding time step counter. A condition needs to be satisfied by the sampling time interval, so as to keep enough modeling accuracy for the spatiotemporally discrete traffic model (see Section 4 for details). Due to the physical structure of urban networks, the original urban roads are directly taken as spatially sampled link segments.

We made the following assumptions:

Assumption 1 *The cycle time of intersection j ($\in J$) can be defined as*

$$c_j = M_j T_j, \quad (1)$$

where T_j is the sampling time interval for intersection j , M_j is an integer, and $M_j \geq 1$. Sampling time intervals and cycle times can be different for different intersections.

Assumption 2 *We assume parallel turning lanes exist in the traffic network. The vehicles getting into a link will run on the link freely without turning separations, until they reach the tail of the waiting vehicle*

queues. Once they reach the tail of the queues, they will be divided to join the separated queues of the turning directions they intend to go.

Now, a spatiotemporally discrete urban traffic model can be derived as follows:

The number of the vehicles in link (u, d) is updated by the input and output average flow rate over sampling time interval T_d at every time step k_d by

$$n_{u,d}(k_d + 1) = n_{u,d}(k_d) + \left(\alpha_{u,d}^e(k_d) - \alpha_{u,d}^l(k_d) \right) \cdot T_d, \quad (2)$$

and consequently we can update the storage capacity as

$$S_{u,d}(k_d) = C_{u,d} - n_{u,d}(k_d), \quad (3)$$

with $C_{u,d}$ the capacity of link (u, d) .

The leaving average flow rate is the sum of the leaving flow rates turning to each output link:

$$\alpha_{u,d}^l(k_d) = \sum_{o \in O_{u,d}} \alpha_{u,d,o}^l(k_d). \quad (4)$$

The leaving average flow rate over T_d is determined by:

$$\alpha_{u,d,o}^l(k_d) = \min \left(\mu_{u,d,o} \cdot g_{u,d,o}(k_d) / T_d, q_{u,d,o}(k_d) / T_d + \alpha_{u,d,o}^a(k_d), \frac{\mu_{u,d,o}}{\sum_{u' \in I_{d,o}} \mu_{u',d,o}} \cdot \frac{C_{d,o} - n_{d,o}(k_d)}{T_d} \right), \quad (5)$$

where $\mu_{u,d,o}$ is the saturation flow rate that can leave link (u, d) turning to link (d, o) depending on the physical structure of link (u, d) (i.e. the allocation of the lanes for traffic flows turning left, right, and going through). A constant $\mu_{u,d,o}$ corresponds to non-shared lanes for leaving flows of different directions; a time-variant $\mu_{u,d,o}$ corresponds to shared lanes. The leaving flow rate is the minimum value of three flow rate values, average saturated flow rate, average unsaturated flow rate, and average over-saturated flow rate, which are given respectively by the three formulas in (5). The first term calculates the average saturated flow rate, which depends on the saturation flow rate $\mu_{u,d,o}$ and the green time duration $g_{u,d,o}$; the second term calculates the average unsaturated flow rate based on the vehicles waiting in and arriving the queues; the third term calculates the average over-saturated flow rate depending on the proportional storage capacity of the downstream link. The inflow from one direction will affect the inflows from the other directions, especially when the downstream storage capacity is limited. By allocating the storage capacity of the downstream link like this, the conflict among different inflows can be approximately addressed.

The number of vehicles waiting in the queue turning to link (d, o) is updated as

$$q_{u,d,o}(k_d + 1) = q_{u,d,o}(k_d) + \left(\alpha_{u,d,o}^a(k_d) - \alpha_{u,d,o}^l(k_d) \right) \cdot T_d. \quad (6)$$

Here we used the Assumption 2 that the vehicles getting into a link do not separate for their turning directions; they run on the link freely until they reach the tail of the waiting vehicle queues, and then

they will join the queues of the turning direction they intend to go. Thus, the number of waiting vehicles in link (u, d) is

$$q_{u,d}(k_d) = \sum_{o \in O_{u,d}} q_{u,d,o}(k_d) . \quad (7)$$

The queues for each direction are calculated vertically, but the number of vehicles arriving to the back of the queues is computed horizontally, for the vehicles usually do not separate for the turning directions before they reach the queues. In [12], vertical queuing approach is applied, which considers the vehicles vertically queue on stop-lines. The flow rate entering link (u, d) will arrive at the end of the queues after a time delay

$$\tau(k_d) = \frac{(C_{u,d} - q_{u,d}(k_d)) \cdot l_{\text{veh}}}{N_{u,d}^{\text{lane}} \cdot v_{u,d}^{\text{free}} \cdot T_d} . \quad (8)$$

Then the delayed flow rate arriving at the end of queues can be obtained by

$$\alpha_{u,d}^a(k_d) = \frac{T_d - \gamma(k_d)}{T_d} \cdot \alpha_{u,d}^e(k_d - \delta(k_d)) + \frac{\gamma(k_d)}{T_d} \cdot \alpha_{u,d}^e(k_d - \delta(k_d) - 1) , \quad (9)$$

where

$$\delta(k_d) = \text{floor} \left\{ \frac{\tau(k_d)}{T_d} \right\} , \quad \gamma(k_d) = \text{rem} \{ \tau(k_d), T_d \} , \quad (10)$$

i.e. $\delta(k_d)$ is the largest integer smaller than or equal to $\frac{\tau(k_d)}{T_d}$, and $\gamma(k_d)$ is the remainder, as shown in Fig. 2. In Section 3, we will illustrate in detail how to sample the traffic model with a continuous time delay into a discrete-time model, and how to deal with the time delay so as to obtain a discrete time delay.

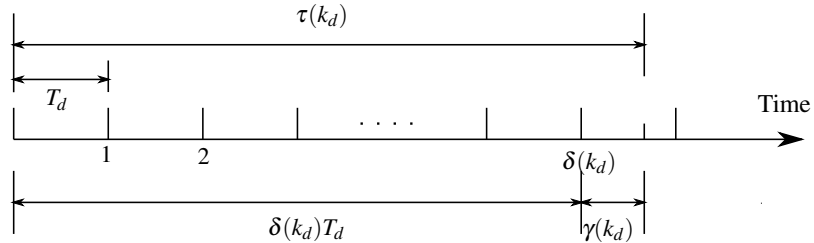


Figure 2. Illustration for the time delay

Before reaching the tail of the waiting queues in link (u, d) , the flow rate of arriving vehicles need to be divided by multiplying it with the turning rates:

$$\alpha_{u,d,o}^a(k_d) = \beta_{u,d,o}(k_d) \cdot \alpha_{u,d}^a(k_d) . \quad (11)$$

The flow rate entering link (u, d) is made up from the flow rates from all the input links:

$$\alpha_{u,d}^e(k_d) = \sum_{i \in I_{u,d}} \alpha_{i,u,d}^1(k_d) . \quad (12)$$

If $c_d \neq c_u$, then $\alpha_{i,u,d}^1(k_u)$ is the leaving flow rate provided by the upstream link, thereafter $\alpha_{i,u,d}^1(k_d)$ cannot be directly obtained from upstream links. Thus, synchronization between the intersections needs to be further addressed, as Section 2.2 illustrates..

2.2 Synchronization between two intersections

In (12), the flow rate entering link (u, d) is provided by the combination of the flow rates leaving the upstream links. According to Assumption 1, we can have different sampling time intervals between upstream and downstream intersections (i.e. $T_u \neq T_d$). Thus, the simulation time steps for the entering flow and the leaving flow may be not equal to each other. Therefore, in order to synchronize the traffic flows in the links connecting to the upper and the downstream intersections, it is necessary to synchronize the leaving and entering flow rates [23]. First of all, a least common multiple time interval is defined as

$$T_{\text{lcm}} = N_j \cdot c_j \quad \text{for all } j \in J, \quad (13)$$

with N_j an integer. Then, in each time interval T_{lcm} , we recast the flow rates expressed in the timing of intersection u into the timing of intersection d . First, we transform the discrete-time leaving flow rates from the upstream links into continuous time using a zero-order hold strategy, as

$$\tilde{\alpha}_{i,u,d}^1(t) = \alpha_{i,u,d}^1(k_u), \quad k_u \cdot T_u \leq t < (k_u + 1) \cdot T_u, \quad (14)$$

and then we sample them again to obtain the average flow rates in time step k_d so that can be used by the downstream link:

$$\alpha_{i,u,d}^e(k_d) = \frac{1}{T_d} \int_{k_d \cdot T_d + \Delta c_{u,d}}^{(k_d+1) \cdot T_d + \Delta c_{u,d}} \tilde{\alpha}_{i,u,d}^1(t) dt, \quad (15)$$

where $\Delta c_{u,d}$ represents the offset time between the cycle times of the upstream and the downstream intersections at the beginning of a control time step. Then, the flow rate entering link (u, d) can be computed by

$$\alpha_{u,d}^e(k_d) = \sum_{i \in I_{u,d}} \alpha_{i,u,d}^e(k_d). \quad (16)$$

The values of the offsets depend greatly on the structure of urban traffic networks. In general, offsets can be designed to maintain maximum green bandwidths for the mainlines in urban traffic networks.

3 Discrete time delay

In this paper, the urban traffic model is a discrete-time model with a discrete time delay, during which a vehicle travels from the beginning of the road until it reaches the queues waiting in the road. By applying the method for sampling a continuous-time system into a discrete-time system [24], we give a proof on obtaining the discrete time delay for the spatiotemporally discrete urban traffic model.

In [24], the theory is given for sampling a continuous-time system with delay into a discrete-time system with discrete-time delay. It is summarized as follows:

Let a linear continuous time-invariant system with time delay $\tau \in \mathbb{R}^+$ be described by¹

$$\dot{\mathbf{X}}(t) = \mathbf{A}\tilde{\mathbf{X}}(t) + \mathbf{B}\tilde{\mathbf{U}}(t - \tau), \quad (17)$$

¹: represents a continuous variable.

where \mathbf{A} and \mathbf{B} are coefficient matrices. Let us now sample this system using a sampling period T . Define

$$\delta = \text{floor} \left\{ \frac{\tau}{T} \right\}, \quad \gamma = \text{rem} \{ \tau, T \}, \quad (18)$$

where $\text{floor}\{x\}$ refers to the largest integer smaller than or equal to x , and $\text{rem}\{x, y\}$ is the remainder of the division of x by y . So δ is an integer, and the time delay τ can be expressed as

$$\tau = \delta \cdot T + \gamma \quad 0 \leq \gamma < T. \quad (19)$$

If the input of the system ($\tilde{\mathbf{U}}(t)$) is assumed to be piece-wise constant during each sampling time interval, the sampled discrete-time system will be

$$\mathbf{X}(k+1) = \Phi \mathbf{X}(k) + \Gamma_0 \mathbf{U}(k-\delta) + \Gamma_1 \mathbf{U}(k-\delta-1), \quad (20)$$

where

$$\Gamma_0 = \int_0^{T-\gamma} e^{\mathbf{A}s} \mathbf{d}s \mathbf{B} \quad (21)$$

$$\Gamma_1 = e^{\mathbf{A}(T-\gamma)} \int_0^{\gamma} e^{\mathbf{A}s} \mathbf{d}s \mathbf{B}. \quad (22)$$

Applying this method, we can prove the expression of the arriving traffic flow with a discrete-time delay in (9). In a traffic network, the vehicles that enter into a link normally will run with free-flow speed for a certain time, and finally join the tail of the queues. This time period is a time delay that is needed before the vehicles join the queues waiting at the stop-line of the link. Then, the queue length in a link is updated by the number of vehicles leaving the link and the number of delayed vehicles entering the link. The differential equation describing the evolution of the queue length of vehicles going to link (d,o) from link (u,d) can be therefore written as

$$\dot{\tilde{q}}_{u,d,o}(t) = \tilde{\beta}_{u,d,o}(t) \tilde{\alpha}_{u,d}^e(t-\tau) - \tilde{\alpha}_{u,d,o}^1(t), \quad (23)$$

where $\tilde{q}_{u,d,o}(t)$, $\tilde{\beta}_{u,d,o}(t)$, $\tilde{\alpha}_{u,d}^e(t)$ and $\tilde{\alpha}_{u,d,o}^1(t)$ are the continuous variables for the queue length, the traffic flow turning rate, the input traffic flow rate and the output traffic flow rate; it describes that the variation of the queue length equals to the arriving flow rate minus the outflow rate. Let us now assume that the traffic flow turning rate ($\tilde{\beta}_{u,d,o}(t)$), and the traffic flow rate entering or leaving the queue ($\tilde{\alpha}_{u,d}^e(t)$ and $\tilde{\alpha}_{u,d,o}^1(t)$), are all piece-wise constant during the sampling time intervals. Then, according to the addition principle of linear equations, (23) can be divided into two equations, as

$$\dot{\tilde{q}}_{u,d,o}^1(t) = -\tilde{\alpha}_{u,d,o}^1(t) \quad (24)$$

$$\dot{\tilde{q}}_{u,d,o}^2(t) = \tilde{\beta}_{u,d,o}(t) \tilde{\alpha}_{u,d}^e(t-\tau), \quad (25)$$

such that

$$\tilde{q}_{u,d,o}(t) = \tilde{q}_{u,d,o}^1(t) + \tilde{q}_{u,d,o}^2(t). \quad (26)$$

According to the aforementioned theory, we can sample the differential equation (24) into a discrete-time equation. Comparing (24) with (17), we define $A = 0$ and $B = -1$ for (24). Since there is no time delay

in (24), we have $\delta = 0$ and $\gamma = 0$. Then, according to (20), (21), and (22), we have $\Phi = 1$, $\Gamma_0 = -T$ and $\Gamma_1 = 0$, thus (24) is sampled as

$$q_{u,d,o}^1(k+1) = \Phi q_{u,d,o}^1(k) + \Gamma_0 \alpha_{u,d,o}^1(k). \quad (27)$$

Similarly, we can sample differential equation (25) with a time delay τ into a discrete-time equation with a discrete-time delay. If we assume that the time delay τ will vary slowly with time t , then according to (18) and (19) we approximately have

$$\delta(k) = \text{floor} \left\{ \frac{\tau(k)}{T} \right\}, \quad \gamma(k) = \text{rem} \{ \tau(k), T \}, \quad (28)$$

Next, comparing (25) with (17), we can define $A_\tau = 0$ and $B_\tau = 1$ for (25). Then, according to (20), (21), and (22), (25), we have $\Phi_\tau = 1$, $\Gamma_0 = T - \gamma(k)$, and $\Gamma_1 = \gamma(k)$, and therefore (25) is sampled as

$$\begin{aligned} q_{u,d,o}^2(k+1) = & \Phi_\tau q_{u,d,o}^2(k) + \beta_{u,d,o}(k) (\Gamma_0 \alpha_{u,d}^e(k - \delta(k)) \\ & + \Gamma_1 \alpha_{u,d}^e(k - \delta(k) - 1)). \end{aligned} \quad (29)$$

Therefore, by adding (27) and (29) together, we derive

$$\begin{aligned} q_{u,d,o}(k+1) = & q_{u,d,o}(k) - T \alpha_{u,d,o}^1(k) + \beta_{u,d,o}(k) ((T - \gamma(k)) \alpha_{u,d}^e(k - \delta(k)) \\ & + \gamma(k) \alpha_{u,d}^e(k - \delta(k) - 1)), \end{aligned} \quad (30)$$

and, comparing (30) with (6) and (11), the arriving average traffic flow at the tail of the queues is therefore proved to be

$$\alpha_{u,d}^a(k) = \frac{T - \gamma(k)}{T} \alpha_{u,d}^e(k - \delta(k)) + \frac{\gamma(k)}{T} \alpha_{u,d}^e(k - \delta(k) - 1). \quad (31)$$

This motivates equation (9).

4 CFL condition for urban traffic models

The Courant-Friedrichs-Lewy condition (CFL condition) [22] is a necessary condition for convergence when solving certain partial differential equations (PDEs) (usually hyperbolic PDEs) numerically. The CFL condition for one dimensional case can be expressed as

$$\frac{v \Delta t}{\Delta x} \leq C, \quad (32)$$

where v is the velocity of flow dynamics, Δt is the time step size, Δx is the spatial step size, and C is a constant scale parameter. Equation (32) makes sure that the time step must be less than a certain value, otherwise the simulation will produce wildly incorrect results.

CFL condition is an important condition for traffic models, and has been used by many models for both freeways and urban roads, e.g. CTM [11] and LTM [12, 13]. In the following context, in order to guarantee the stability of the spatiotemporally discrete urban traffic model, we will prove in theory the existence of the CFL condition for urban road networks.

For a spatiotemporally discrete urban traffic model, we know that the number of vehicles that can leave link $(u, d) \in L$ during time step k_d should not exceed the number of vehicles on this link, i.e.

$$\alpha_{u,d}^1(k_d)T_d \leq n_{u,d}(k_d) \leq C_{u,d}, \quad (33)$$

where the number of vehicles on link (u, d) is bounded by its storage capacity $C_{u,d}$, and the average leaving traffic flow $\alpha_{u,d}^1(k_d)$ is given by (4) and (5).

Then, by dividing the number of vehicles on link (u, d) into two parts, the number of vehicles in the queue ($q_{u,d}(k_d)$) and the number of vehicles running freely on the link ($f_{u,d}(k_d)$), as Fig. 3 shows, we have

$$T_d \leq \frac{n_{u,d}(k_d)}{\alpha_{u,d}^1(k_d)} = \frac{q_{u,d}(k_d) + f_{u,d}(k_d)}{\alpha_{u,d}^1(k_d)}. \quad (34)$$

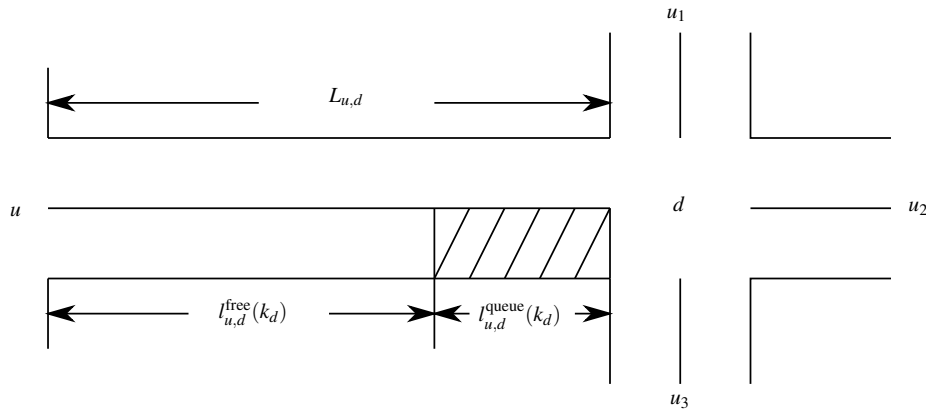


Figure 3. Illustration of the division of vehicles in link (u,d) in freely running vehicles and vehicles waiting in queues

According to (4) and (5), we know that the average leaving traffic flow is larger than or equal to the arriving traffic flow at the end of the queues, i.e. $\alpha_{u,d}^a(k_d) \leq \alpha_{u,d}^1(k_d)$, in most of the situations except when spillback occurs in the downstream links and the link (u, d) is almost congested. For most of the situations, we can assume that the vehicles freely run on link (u, d) with constant flow rate, $\alpha_{u,d}^a(k_d)$, before joining the tail of the vehicle queues, i.e. $\alpha_{u,d}^{\text{free}} = \alpha_{u,d}^a(k_d)$. Consequently, the flow rate for the free-running vehicles is smaller than or equal to the average flow rate of the leaving vehicles from link (u, d) , i.e. $\alpha_{u,d}^{\text{free}}(k_d) \leq \alpha_{u,d}^1(k_d)$. In addition, the flow rate for the vehicles moving in queues is also smaller than or equal to the average flow rate of the leaving vehicles from link (u, d) , i.e. $\alpha_{u,d}^{\text{queue}}(k_d) \leq \alpha_{u,d}^1(k_d)$. Hence, (34) can be further written into

$$\begin{aligned} T_d &\leq \frac{q_{u,d}(k_d)}{\alpha_{u,d}^{\text{queue}}(k_d)} + \frac{f_{u,d}(k_d)}{\alpha_{u,d}^{\text{free}}(k_d)} \\ &= \frac{\rho_{u,d}^{\text{queue}}(k_d)l_{u,d}^{\text{queue}}(k_d)}{\alpha_{u,d}^{\text{queue}}(k_d)} + \frac{\rho_{u,d}^{\text{free}}(k_d)l_{u,d}^{\text{free}}(k_d)}{\alpha_{u,d}^{\text{free}}(k_d)} \end{aligned}$$

$$= \frac{l_{u,d}^{\text{queue}}(k_d)}{v_{u,d}^{\text{queue}}(k_d)} + \frac{l_{u,d}^{\text{free}}(k_d)}{v_{u,d}^{\text{free}}}, \quad (35)$$

where $\rho_{u,d}^{\text{queue}}(k_d)$ and $\rho_{u,d}^{\text{free}}(k_d)$ are the density of the queue and the density of the free-running traffic flow on link (u,d) at time step k_d respectively. Furthermore, because the length of link (u,d) is equal to the sum of the queue length and the free-running link length, i.e. $l_{u,d}^{\text{queue}}(k_d) + l_{u,d}^{\text{free}}(k_d) = L_{u,d}$, and the average speed of the vehicles waiting in queues is bounded as $0 \leq v_{u,d}^{\text{queue}}(k_d) \leq v_{u,d}^{\text{free}}$, we have

$$\frac{L_{u,d}}{v_{u,d}^{\text{free}}} \leq \frac{l_{u,d}^{\text{queue}}(k_d)}{v_{u,d}^{\text{queue}}(k_d)} + \frac{l_{u,d}^{\text{free}}(k_d)}{v_{u,d}^{\text{free}}} \leq \frac{L_{u,d}}{v_{u,d}^{\text{queue}}(k_d)}, \quad (36)$$

where the lower bound and the upper bound correlate to two extreme situations on link (u,d) , i.e. free-flow and congested situations. Hence, according to (35) and (36), we can derive a sufficient condition for the sampling time interval T_d of the model, as

$$T_d \leq \frac{L_{u,d}}{v_{u,d}^{\text{free}}}, \quad (37)$$

which is exactly a CFL condition. The condition can be interpreted intuitively as requiring that the distance $v_{u,d}^{\text{free}}T_d$ traveled by a traffic flow in one time step should not exceed one spatial step $\Delta x = L_{u,d}$, or equivalently that the numerical traffic flow speed $L_{u,d}/T_d$ should be at least as fast as the physical traffic flow speed $v_{u,d}^{\text{free}}$. By satisfying this CFL condition, we can make sure that all the traffic flow perturbations can be captured by the spatiotemporally discrete model, and no traffic flow is created or disappear during the evolution of the model. In practice, a CFL condition can be used as a criterion for selecting proper sampling time intervals for the spatiotemporally discrete traffic model.

However, for urban intersections, the sampling time intervals of intersection d do not only depend on the link (u,d) , but also on the rest of the links connected to this intersection. We define $U_d \subset J$ as the set of the upstream intersections of intersection $d \in J$. Therefore, to guarantee that the spatiotemporally discrete urban traffic model can correctly represent the urban traffic dynamics, the simulation time interval T_d (i.e. sampling time interval) needs to satisfy condition:

$$T_d \leq \min_{u' \in U_d} \left(\frac{L_{u',d}}{v_{u',d}^{\text{free}}} \right). \quad (38)$$

In order to keep the model of each intersection balance between the modeling accuracy and the computational complexity, different sampling time intervals need to be selected for different intersections according to their specific intersection CFL conditions.

5 Model Assessment

In this section, we evaluate the effectiveness of the spatiotemporally discrete urban traffic model, and analyze its sensitivity from a control point of view. Experiments are designed to demonstrate how the Total Time Spent (TTS, frequently selected as traffic control performance criterion) will change by varying green time lengths of traffic signals. The urban road network considered in this evaluation is

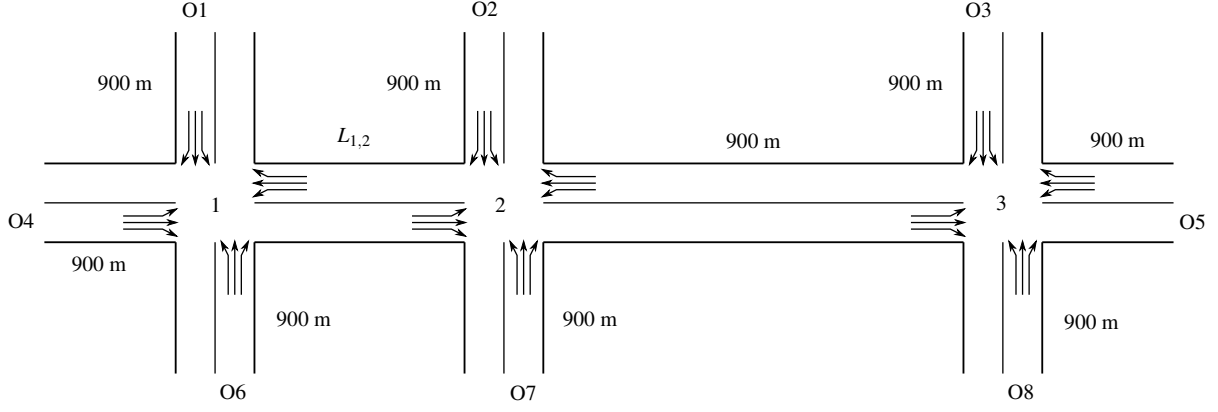


Figure 4. Layout of the urban road network of the case study

Table 1. Fixed-time control setup for the traffic signals

Intersection	Phase 1 (s)	Phase 2 (s)	Cycle time (s)
1	45	45	90
2	$g_{2,1}$	$90 - g_{2,1}$	90
3	$g_{3,1}$	$90 - g_{3,1}$	90

shown in Fig. 4. It is a simple urban road network with 3 intersections, and 8 origins. The origins, marked as “Ox”, are the origin nodes where traffic flows enter the network. The evaluation performance criterion is the TTS, which is the accumulated time spent by all the vehicles in a region of the road network for the entire simulation time.

The lengths of the roads in the network are listed in Fig. 4, and each road has 3 lanes. The anticipating turning rates β are taken to be constant, i.e. 0.33 for left turn, through turn, and right turn respectively. The saturation flow rates μ are 1800 veh/h, 1600 veh/h, and 1500 veh/h respectively for moving through, turning left, and turning right in each link. The average vehicle length l_{veh} is set to 7 m, and the free-flow speed $v_{u,d}^{free}$ is 50 km/h.

The spatiotemporally discrete urban traffic model will be evaluated under the following traffic scenarios:

- *Scenario 1:* The length of link (1,2) is 450m, the network input flow rates of the network are set to be equal to each other and constant in time, i.e. $\alpha_{o_x}=2000$ veh/h for all origins.
- *Scenario 2:* The length of link (1,2) is 450m, the network input flow rates of the network are set to be constant in time, and $\alpha_{o_4}=\alpha_{o_5}=2000$ veh/h, $\alpha_{o_1}=\alpha_{o_2}=\alpha_{o_3}=\alpha_{o_6}=\alpha_{o_7}=\alpha_{o_8}=500$ veh/h).
- *Scenario 3:* The length of link (1,2) is 150m, the network input flow rates of the network are set to be equal to each other and constant in time, i.e. $\alpha_{o_x}=2000$ veh/h for all origins.

Fixed-time control is executed for each intersection, where the phases, the cycle times, and the green time lengths are all constant during each simulation. The phases and their order for all the intersections are given in Fig. 5. The green time lengths and cycle times are shown in Table 1, where the symbol $g_{j,i}$ stands for the green time length of the i th phase for intersection j . In order to evaluate how the evaluation performance (TTS) changes with the settings of the traffic signals, we assess the TTS by

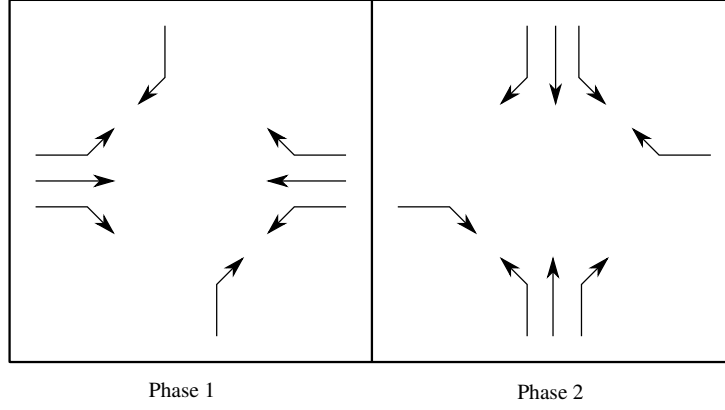


Figure 5. Intersection traffic signal phases

Table 2. CFL conditions for each intersection under different traffic scenarios

Scenario	Intersection 1	Intersection 2	Intersection 3
1 & 2	$T_d \leq 32$ s	$T_d \leq 32$ s	$T_d \leq 64$ s
3	$T_d \leq 10$ s	$T_d \leq 10$ s	$T_d \leq 64$ s

running the spatiotemporal urban traffic model with different fix-time control schemes for Intersection 2 and 3, i.e. we allow the green time lengths of intersection 2 and 3 to change within a given time region: $g_{2,1}, g_{3,1} \in \{15, 20, 25, 30, 35, 40, 45, 50, 55, 60, 65, 70, 75\}$. The lower bound and the upper bound for a green time duration is 15 s and 75 s, and $g_{2,2}$ and $g_{3,2}$ change accordingly with $g_{2,1}$ and $g_{3,1}$, due to the cycle time constraint of each intersection. That is to say we let the green timings of Intersection 2 and 3 enumerate all the possible values between the maximum and minimum green times, so as to evaluate how the green timings will affect the network performance. The proposed spatiotemporally discrete traffic model is sampled by different sampling time intervals (simulation time intervals), i.e. $T = 1$ s, 30 s, and 90 s respectively. According to the CFL condition for urban traffic models in Section 4, the upper bounds of the sampling time intervals for each intersection under different traffic scenarios are given by Table 2. Then, for each set-up of the traffic signals, all the sampled spatiotemporally discrete traffic models are run for the same period of time (30 min).

For Scenario 1, according to Table 2, when $T = 30$ s, the urban CFL conditions are satisfied in all the three intersections; when $T = 90$ s, the urban CFL conditions are violated for every intersection. The results are shown in Fig. 6 and Fig. 7 for the TTS of the entire network and for the TTS of link (1,2), in which the urban CFL condition is easier to be violated. From Fig. 6 and Fig. 7, we can see that the spatiotemporally discrete traffic model can describe a more detailed variation of the TTS changing with the green time lengths, when the sampling time interval is small. For $T = 1$ s and $T = 30$ s, the shapes of the TTS curves are very similar to each other for both the entire network and the single link (1,2). Generally speaking, the larger the sampling time interval is, the faster the model will run. For the spatiotemporally discrete traffic models with sampling time intervals of 1 s and 30 s, the time needed to run the model are 5.6 s and 0.4 s respectively. Consequently, the spatiotemporally discrete model with $T = 30$ s is a better choice for urban traffic network control, because it can guarantee almost the same performance as the spatiotemporally discrete model with $T = 1$ s, but requires less computing time. For the spatiotemporally discrete model with sampling time 90 s, the time needed to run the model is even

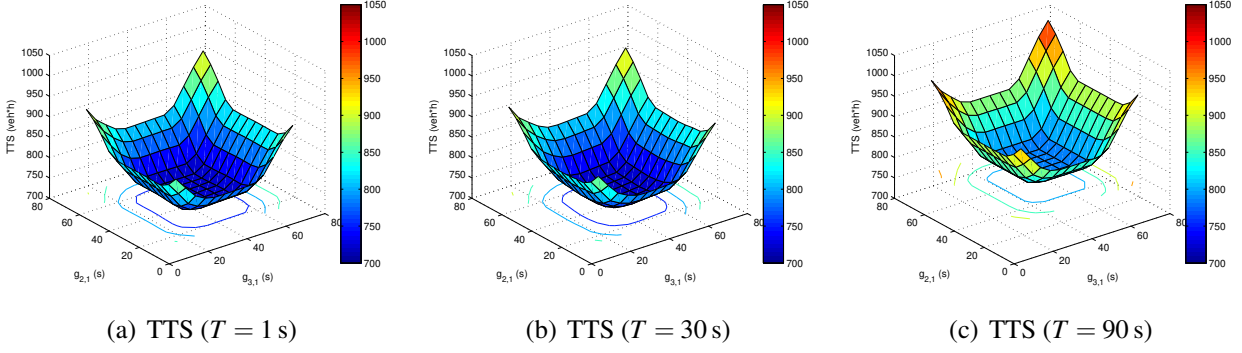


Figure 6. TTS of the network for spatiotemporally discrete model with different sampling time intervals under Scenario 1

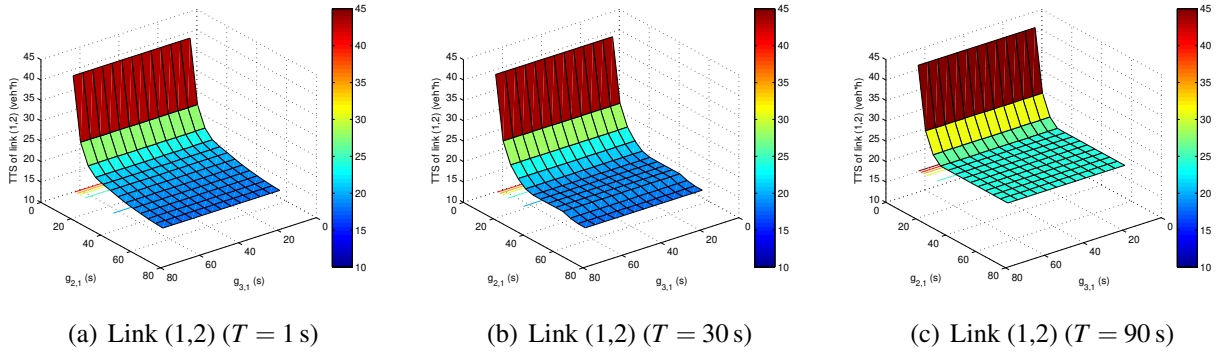


Figure 7. TTS of link (1,2) for spatiotemporally discrete model with different sampling time intervals under Scenario 1

less: 0.2 s. However, the sampling time then becomes too large and it violates the CFL condition. Thus, the model fails to describe the correct variation of the traffic phenomena. Indeed, in Fig. 6(c), the values of the TTS become much higher than those of the spatiotemporally discrete model with $T = 1$ s and $T = 30$ s. In Fig. 7(c), the TTS curve becomes distorted, which cannot capture the accurate variation of TTS values anymore. Therefore, even though the spatiotemporally discrete model with $T = 90$ s is very fast, but it does not have sufficient accuracy to be used as a control model. Consequently, in this case study, the spatiotemporally discrete urban traffic model with sampling time $T = 30$ s is comparatively more suitable for use as a prediction model for the urban traffic controllers, as it gives a good trade-off between the modeling accuracy and the computational complexity.

For Scenario 2, the same conclusions can be derived from Fig. 8 and Fig. 9, i.e. the spatiotemporally discrete urban traffic model with sampling time $T = 30$ s balances the modeling accuracy and the computational complexity best. But, due to the different network input flow rates, Fig. 8 gives different shape of the TTS for the network from that of Fig. 6, from which we can see that the two figures give different optimal green time regions for Scenario 1 and 2. The reason for this phenomenon is that the network

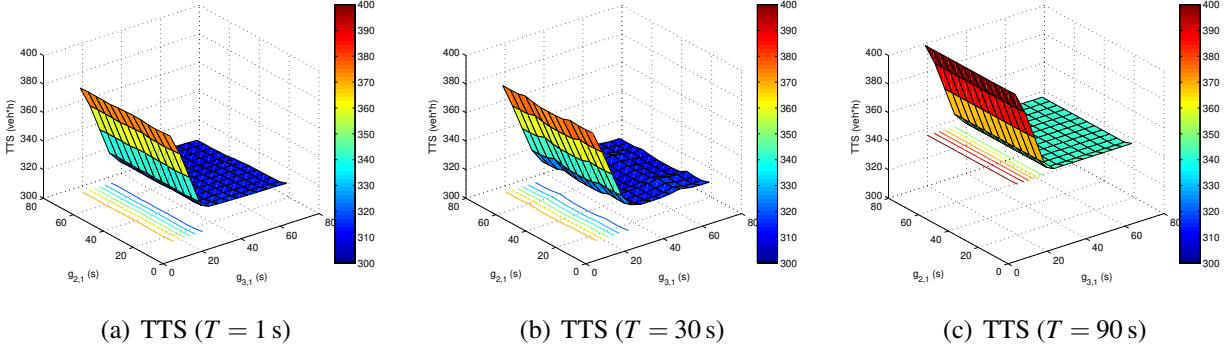


Figure 8. TTS of the network for spatiotemporally discrete model with different sampling time intervals under Scenario 2

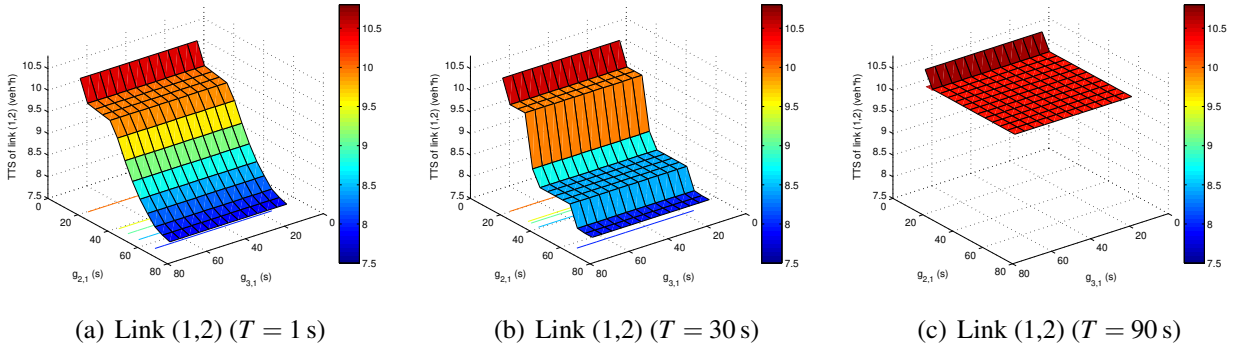


Figure 9. TTS of link (1,2) for spatiotemporally discrete model with different sampling time intervals under Scenario 2

input flow rates are different for Scenario 1 and 2, which makes the network input traffic demands are balanced in Scenario 1, but imbalanced in Scenario 2. The differences between Fig. 6 and 8 show that optimal green timing can be found based on the proposed spatiotemporal urban traffic model for different network traffic demands. In Fig. 7(c), it happens that the outflow of link (1,2) is not changing with the increase of the green timing $g_{2,1}$, which results in the flat surface on the figure. The reason for this phenomenon is that the CFL condition is violated in link (1,2), i.e. the outflow is restricted by the storage capacity of the link and stays constant, no matter how the expected outflow is regulated by adjusting the green timings. Similar phenomenon is detected in Fig. 9(c), but the flat area is more obvious due to the reduction in network input traffic flows.

For Scenario 3, the length of link (1,2) and link (2,1) is reduced from 450 m to 150 m, so the CFL condition is even tighter for Intersection 1 and 2, as Table 2 shows. Thus, even though the sampling time interval is selected as $T = 30$ s, the CFL condition is also violated. In such a condition, the comparisons of the TTS of the entire network and of the TTS of link (1,2) are shown in Fig. 10 and Fig. 11. Since the CFL condition is violated when $T = 30$ s, Fig. 11(b) shows that the spatiotemporally discrete model

fails to follow the trend of the curve in Fig. 11(a). As the CFL condition suggests, the shorter the network links are, and the higher the free-flow speed is, the smaller a sampling time interval is needed to provide enough accuracy for the spatiotemporally discrete urban traffic model. Since the CFL condition is violated in both Fig. 11(c) and Fig. 11(b), the flat surfaces emerge in both the figures. Moreover, in Fig. 11(c), the flat area is even larger than in the previous two scenarios, due to increment of the degree that the CFL is violated.

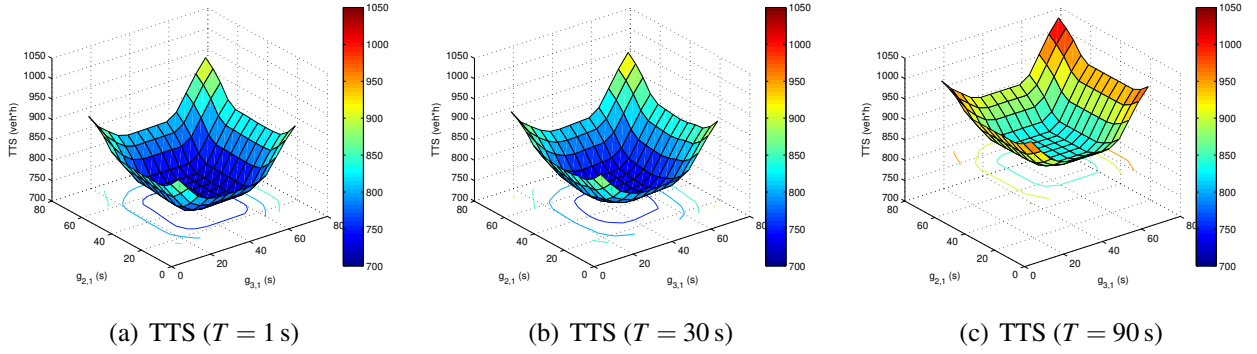


Figure 10. TTS of the network for the spatiotemporally discrete model with different sampling time intervals under Scenario 3

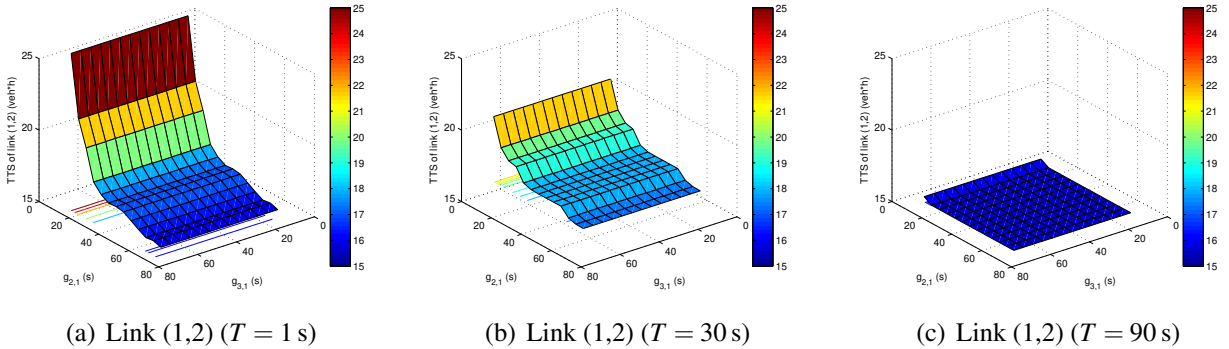


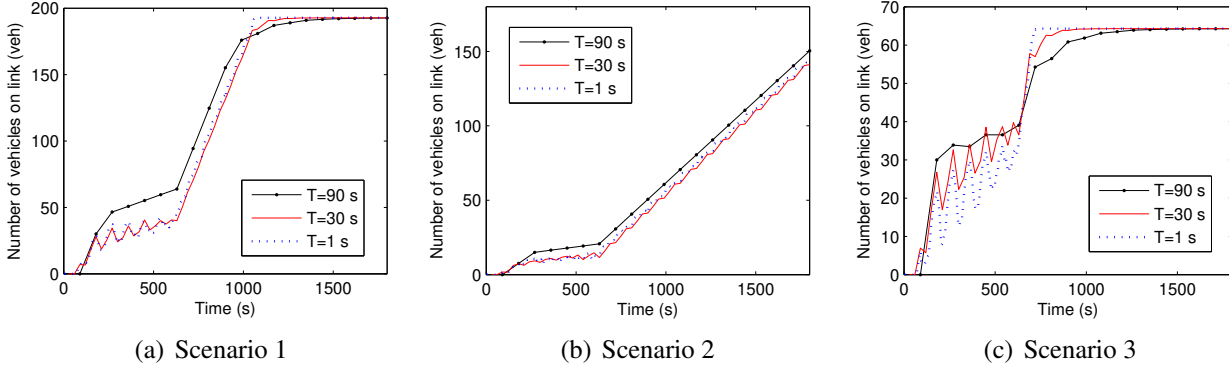
Figure 11. TTS of link (1,2) for the spatiotemporally discrete model with different sampling time intervals under Scenario 3

In order to summarize Fig. 6 to 11, the results are listed again in Table 3 for $g_{2,1} = 75$ s and $g_{3,1} = 15$ s in all the scenarios, and the errors are given for each scenario compared to the results with $T = 1$ s.

From the results of Fig. 6, 8, and 10, green times can be selected in the optimal green time regions of different traffic scenarios, i.e. $g_{2,1} = 45$ s and $g_{3,1} = 45$ s for Scenario 1 and 3, $g_{2,1} = 45$ s and $g_{3,1} = 75$ s for Scenario 2. These green times are approximately taken as the optimal green times for each traffic scenario. When the approximated optimal green times are set for each traffic scenario, the evolution

Table 3. The TTS in all the scenarios for $g_{2,1} = 75$ s and $g_{3,1} = 15$ s

Sampling time	TTS of network (veh·h)			TTS of link (1,2) (veh·h)		
	1s	30s	90s	1s	30s	90s
Scenario 1	874	878 (0.5%)	951 (8.8%)	12.5	12.9 (3.2%)	19.0 (52.0%)
Scenario 2	314	315 (0.3%)	339 (8.0%)	7.5	7.7 (2.7%)	10.6 (41.3%)
Scenario 3	882	891 (1.0%)	978 (10.9%)	16.5	17.1 (3.6%)	15.0 (-9.1%)

**Figure 12. The evolution of the number of vehicles in link (2,1)**

of the number of vehicles in link (2,1) is shown in Fig. 12 for different sampling time intervals. The storage capacity $C_{2,1}$ of link (2,1) is 193 veh for Scenario 1 and 2, and 64 veh for Scenario 3. As the figure illustrates, for Scenario 1 and 3, there exists spillback on link (2,1), where the number of vehicles in link (2,1) reaches the storage capacity, and as a result the departures from upstream links will be blocked. However, when $T = 90$ s, due to the low accuracy of the spatiotemporally discrete model, the spillback cannot occur as fast as the spillback when $T = 1$ s and $T = 30$ s. For Scenario 2, as the network input traffic flows are comparatively low, there is no spillback happens.

6 Conclusions

According to the requirement of real-time model-based traffic control strategies, urban traffic models that are both accurate and fast are needed. Consequently, in this paper, a macroscopic spatiotemporally discrete urban traffic model with a variable sampling time interval is proposed for model-based control strategies. By varying the sampling time interval, the spatiotemporally discrete traffic model allows us to balance the modeling accuracy and the computational complexity, and thus allows to search for the best trade-off based on the specific control requirements. This model is able to describe the time delay taken by the vehicles before joining the end of the queues in a link, which makes it possible to estimate the arriving traffic flow in the link under unsaturated traffic scenario. In addition, an urban traffic CFL condition is deduced for the spatiotemporally discrete urban traffic model, which is a sufficient condition to guarantee the modeling accuracy of the prediction model.

Experiments have been performed to verify whether the model has sufficient descriptive power to reproduce the necessary phenomena for traffic control under the situations that the CFL condition is

violated and not violated, and whether the computation speed of the model is high enough. The experiment results illustrate that the macroscopic spatiotemporally discrete urban traffic model is suited for use in model-based control strategies, and the higher the sampling frequency is, the more accurate the spatiotemporally discrete model will be, but also the more computation time is needed. When the CFL condition is violated, the spatiotemporally discrete model failed to provide correct traffic state prediction. Therefore, by selecting a proper sampling time interval under the guidance of the urban CFL condition, a trade-off can be made between the computation time and the accuracy for the spatiotemporally discrete traffic model. The deduced urban traffic CFL condition can be applied as a guideline for selecting the sampling time interval and the sampling space distance of spatiotemporally discrete urban traffic models.

In the future, model-based urban traffic controllers will be further established and tested for large-scale urban traffic networks based on the spatiotemporally discrete model. Moreover, the results of this paper will be further investigated for urban traffic control by comparing the proposed model with other well known models.

Acknowledgements

This research is supported by National Science Foundation of China (60934007, 61104160, 61203169), China Postdoctoral Science Foundation (2011M500776), Shanghai Education Council Innovation Research Project (12ZZ024), Chinese International Cooperation Project of National Science Committee (Grant No. 71361130012), European COST Actions TU0702 and TU1102, BSIK project “Next Generation Infrastructures (NGI)”, and Transport Research Centre Delft.

References

- [1] Hoogendoorn SP, Bovy PHL. State-of-the-art of vehicular traffic flow modelling. Proceedings of the Institution of Mechanical Engineers, Part I: Journal of Systems and Control Engineering. 2001;215(4):283-303.
- [2] Lighthill MJ, Whitham GB. On kinematic waves. II. A theory of traffic flow on long crowded roads. Proceedings of the Royal Society of London Series A, Mathematical and Physical Sciences. 1955;229(1178):317-45.
- [3] Payne HJ. Models of freeway traffic and control. Mathematical Models of Public Systems. 1971;1(1):51-61.
- [4] Daganzo CF. Requiem for second-order fluid approximations of traffic flow. Transportation Research Part B. 1995;29(4):277-86.
- [5] Papageorgiou M. Some remarks on macroscopic traffic flow modelling. Transportation Research Part A: Policy and Practice. 1998;32(5):323-9.
- [6] Gazis DC, Potts RB. The oversaturated intersection. In: Proceedings of the 2nd International Symposium on Traffic Theory; 1963. .

- [7] Diakaki C, Papageorgiou M, Aboudolas K. A multivariable regulator approach to traffic-responsive network-wide signal control. *Control Engineering Practice*. 2002;10(2):183-95.
- [8] Aboudolas K, Papageorgiou M, Kouvelas A, Kosmatopoulos E. A rolling-horizon quadratic-programming approach to the signal control problem in large-scale congested urban road networks. *Transportation Research Part C: Emerging Technologies*. 2010;18(5):680-94.
- [9] Barisone A, Giglio D, Minciardi R, Poggi R. A macroscopic traffic model for real-time optimization of signalized urban areas. In: *Proceedings of the 41st IEEE Conference on Decision and Control*. Las Vegas (NV), USA; 2002. p. 900-3.
- [10] Dotoli M, Fanti MP, Meloni C. A signal timing plan formulation for urban traffic control. *Control Engineering Practice*. 2006;14(11):1297-311.
- [11] Daganzo CF. The cell transmission model: A dynamic representation of highway traffic consistent with the hydrodynamic theory. *Transportation Research Part B: Methodological*. 1994;28(4):269-87.
- [12] Yperman I, Logghe S, Tampère CMJ, Immers LH. The multi-commodity link transmission model for dynamic network loading. In: *Proceedings of the 85th Annual Meeting of the Transportation Research Board*. 06-1062. Washington D.C., USA; 2006. .
- [13] Tampère CM, Corthout R, Cattrysse D, Immers LH. A generic class of first order node models for dynamic macroscopic simulation of traffic flows. *Transportation Research Part B: Methodological*. 2011;45(1):289-309.
- [14] Richards PI. Shock waves on the highway. *Operations Research*. 1956;4(1):42-51.
- [15] Kashani HR, Saridis GN. Intelligent control for urban traffic systems. *Automatica*. 1983;19(2):191-7.
- [16] van den Berg M, Hegyi A, De Schutter B, Hellendoorn J. A macroscopic traffic flow model for integrated control of freeway and urban traffic networks. In: *Proceedings of the 42nd IEEE Conference on Decision and Control*. Maui (HI), USA; 2003. p. 2774-9.
- [17] Hegyi A. *Model Predictive Control for Integrating Traffic Control Measures [PhD thesis]*. Delft, The Netherlands: Delft University of Technology; 2004.
- [18] van den Berg M, De Schutter B, Hegyi A, Hellendoorn J. Model predictive control for mixed urban and freeway networks. In: *Proceedings of the 83rd Annual Meeting of the Transportation Research Board*. Washington D.C., USA; 2004. Paper 04-3327.
- [19] Lin S, Xi Y. An efficient model for urban traffic network control. In: *Proceedings of the 17th World Congress of the International Federation of Automatic Control*. Seoul, Korea; 2008. p. 14066-71.
- [20] Lin S, De Schutter B, Xi Y, Hellendoorn J. A simplified macroscopic urban traffic network model for model-based predictive control. In: *Proceedings of the 12th IFAC Symposium on Control Transportation Systems*. Redondo Beach (CA), USA; 2009. p. 286-91.

- [21] Lin S, De Schutter B, Xi Y, Hellendoorn H. Efficient network-wide model-based predictive control for urban traffic networks. *Transportation Research Part C*. 2012;24:122-40.
- [22] Courant R, Friedrichs K, Lewy H. On the partial difference equations of mathematical physics. *IBM Journal of Research and Development*. 1967;11(2):215-34.
- [23] Lin S, De Schutter B, Hegyi A, Xi Y, Hellendoorn H. A spatiotemporally discrete urban traffic model. In: *Proceedings of the 18th World Congress of the International Federation of Automatic Control*. Milano, Italy; 2011. p. 10697-702.
- [24] Åström KJ, Wittenmark B. *Computer-Controlled Systems: Theory and Design*. Prentice Hall New York; 1996.